How to cite: *Angew. Chem. Int. Ed.* **2022,** *61,* e202209033
International Edition: doi.org/10.1002/anie.202209033
German Edition: doi.org/10.1002/ange.202209033

Green Chemistry | Hot Paper

A Greener Route to Blue: Solid-State Synthesis of Phthalocyanines

Daniel Langerreiter, Mauri A. Kostiainen, Sandra Kaabel, and Eduardo Anaya-Plaza**

Dedicated to Professor Tomás Torres on the occasion of his 70th birthday

Abstract: Phthalocyanines are important organic dyes with a broad applicability in optoelectronics, catalysis, sensing and nanomedicine. Currently, phthalocyanines are synthetized in high boiling organic solvents, like dimethylaminoethanol (DMAE), which is a flammable, corrosive, and bioactive substance, miscible with water and harmful to the environment. Here we show a new solid-state approach for the high-yielding synthesis of phthalocyanines, which reduces up to 100-fold the amount of DMAE. Through systematic screening of solid-state reaction parameters, carried out by ball-milling and aging, we reveal the influence of key variables—temperature, presence of a template, and the amount and role of DMAE in the conversion of *t*Bu phthalonitrile to tetra-*t*Bu phthalocyanine. These results set the foundations to synthesize these high-performance dyes through a greener approach, opening the field of solid-state synthesis to a wider family of phthalocyanines.

In the past years sustainability and environmentally friendly alternatives of producing and synthesizing chemicals are heavily investigated, aligned with the UN sustainable development goals #6 and #12—clean water and sanitation, and responsible consumption and production, respectively. An emerging greener route to achieve these goals relies on solid-state reactions, where solvent use is avoided or drastically reduced.[1,2] Mechanochemistry in particular[3–5] has gained importance not only in organic or (metallo)-organic synthesis,[6,7] but also in polymer science[8] or material chemistry.[9,10] Synthesis of organic dyes, where water-miscible, high-boiling point solvents are widely used, will particularly benefit from a more environmentally friendly synthesis pathway. Mechanochemical and solid-state synthesis of dyes has the potential to avoid large-scale use of solvents,[11] thus mitigating the threat to water quality and the environment, while bringing economic benefits to industry.

One of the most prominent members among the organic dyes are phthalocyanines (Pcs). They consist of four isoindole units linked through aza-bridges. These macrocycles can host up to 60 different elements in their core. Their extended aromatic structure of 18 delocalized electrons endow them with remarkable and tunable optical properties,[12,13] such as high molar absorptivity in the red-near infrared range (ca. 600–700 nm), and moderate-to-high fluorescence, phosphorescence, and singlet oxygen generation quantum yields.[14] Pcs show a rich chemistry that enables fine tuning of their colloidal properties,[15] as well as their conjugation with other photoactive materials[16–18] or biomolecules.[19–22] Therefore, they are multifunctional molecular materials with applications in optoelectronics,[17,23–25] catalysis,[26–28] sensors,[29] and nanomedicine.[30–35] Traditional Pc synthesis in solution is carried out by cyclotetramerization of the phthalic anhydride, phthaloimide, 1,3-diiminoisoindoles, or phthalonitrile of interest in solvents such as dimethylaminoethanol (DMAE), or alkoxides like lithium 1-pentanolate.[36–40] Catalytic amounts of non-nucleophilic bases such as 1,8-diazabicyclo[5.4.0]undec-7-ene (DBU) are commonly used as catalyst. Pcs have been reported to show crystallographic polymorphism under ball-milling processing,[41] and have been employed in solid-state preparation of composite materials for traditional applications such as catalysis,[42–44] energy conversion[45] and storage,[46,47] and others.[48–51] However, to the extent of our knowledge, the solid-state synthesis of Pcs has not been reported.

Herein we develop a new solid-state synthetic method for Pcs. We selected tetra-*t*Bu Pc (**1**) as model compound and 4-*t*Bu phthalonitrile (**2**) as precursor (Figure 1a), in the presence of equimolar amounts of DMAE. This approach using ball milling (liquid-assisted grinding, LAG)[52,53] and aging[54] reduces the amount of solvent up to 100-fold compared to conventional conditions, typically carried out at ca. 0.2 M in DMAE reflux.[55] The solid-state reaction proceeds at lower temperature, differing from harsh conditions used in molten-state reactions that result in overall low yields,[56–59] and gives a 4-fold increase in Space–Time–Yield (STY). Our results provide a thorough insight into parameters influencing the solid-state synthesis of **1**, committing to a more sustainable chemistry without compromising reaction efficiency.

[*] D. Langerreiter, Prof. M. A. Kostiainen, Dr. S. Kaabel, Dr. E. Anaya-Plaza
Department of Bioproducts and Biosystems,
Aalto University
02150 Espoo (Finland)
E-mail: sandra.kaabel@aalto.fi
eduardo.anaya@aalto.fi

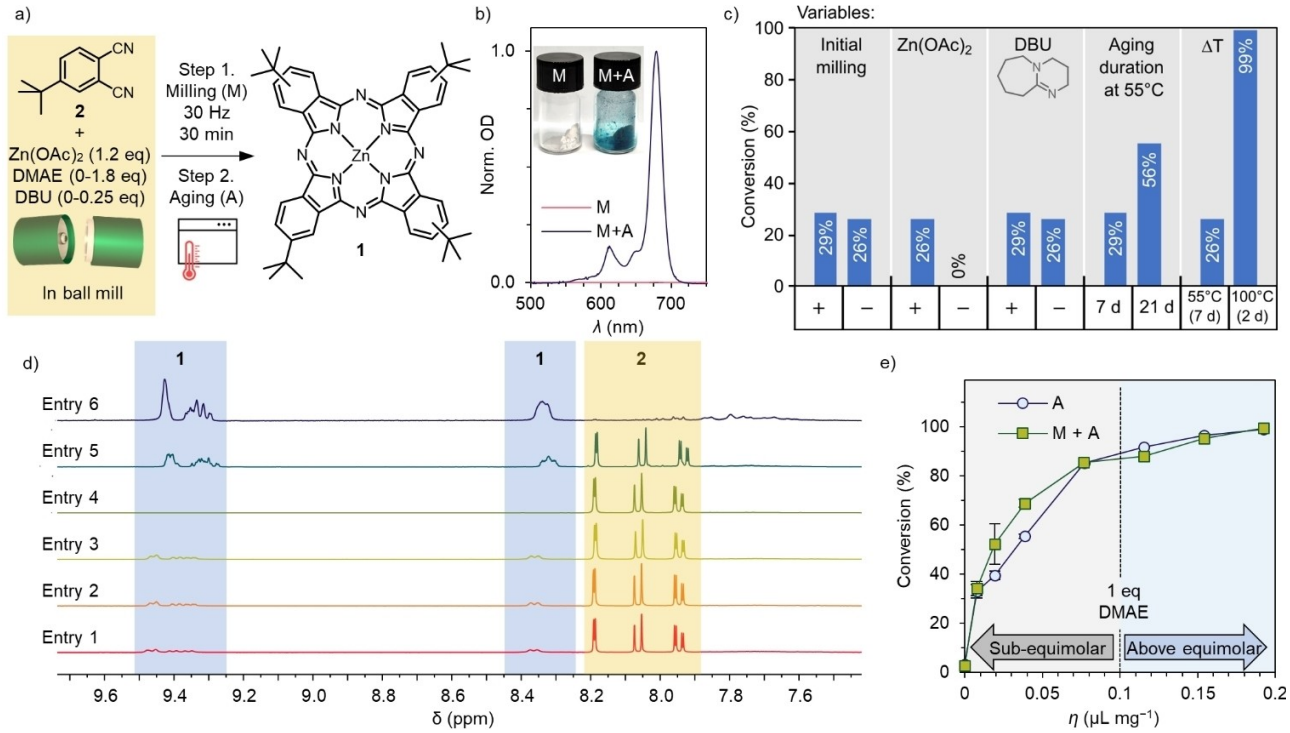

Figure 1. a) The general reaction scheme of solid-state synthesis of **1** combining milling (M) and aging (A). b) UV/Vis spectra showing the normalized absorption of the crude reaction in d_6-DMSO after M (red) and M + A (blue). Inset: photographs of as-obtained samples after M and M + A. c) Screened solid-state reaction parameters and respective conversion as measured by NMR. Full experimental details are shown in Table 1, Entries 1–6. d) Partial ^{1}H NMR spectra of Entry 1–6, showing the aromatic region used for calculating the conversion. Assigned peaks for **1** and **2** are highlighted in blue and yellow, respectively. e) Conversion of **1** depending on the mixing technique (M + A in green squares, A in blue circles) upon increase of DMAE amount from $\eta = 0.0$ to 0.192 μL mg^{-1}. Sub-equimolar and above equimolar ranges of DMAE to **1** are highlighted in grey and blue, respectively. Other parameters were kept constant (i.e. 1.2 equiv of $Zn(OAc)_2$, temperature 100 °C, no DBU, 48 h). Triplicate reactions were carried out for the region $\eta = 0.019$ to 0.077 μL mg^{-1} where mixing effect was observed between M + A and A. The error bars represent the standard deviation.

Initial experiments investigating the formation of **1** during LAG, that is ball milling **2** in the presence of $Zn(OAc)_2$ and a small amount of the liquids DMAE (liquid-to-solid ratio,[60] $\eta = 0.192$ μL mg^{-1}) and DBU ($\eta = 0.039$ μL mg^{-1}) for 30 minutes at 30 Hz, shows no detectable amount of the intensely blue-colored product **1** (Figure 1b). However, when the resulting white paste-like solid was enclosed in screw-cap vials and aged in an oven at 55 °C, deep blue color evolved during a week (Figure 1b), resulting into a 29 % conversion of **2** into **1** (Table 1, Entry 1), determined by ^{1}H NMR in d_6-DMSO (Figure 1c and d). The calculated conversion (see Supporting Information, Figure S1) does not account for potential side reactions, although no other signals are apparent in the aromatic region of the ^{1}H NMR (Figure 1d, Entry 1). Importantly, the measured conversion remains unchanged after 14 days of storing in d_6-DMSO, demonstrating that the reaction is effectively quenched at the measurement conditions. Comparable conversion of 26 % was reached when the reaction was started by simply mixing the reactants in the glass vials

Table 1: Screened parameters for the formation of **1**, and resulting conversions. All reactions were started with 200 mg of **2**, 60 mg of $Zn(OAc)_2$, and DMAE ($\eta = 0.192$ μL mg^{-1}), unless otherwise stated.

Entry	Mixing technique	DBU [μL mg^{-1}]	Aging time [days]	Aging temp. [°C]	Conv. [%]
1	M + A	0.039	7	55	29
2	A	0.039	7	55	26
3	M + A	0	7	55	26
4[a]	M + A	0	7	55	0
5	M + A	0.039	21	55	56
6	M + A	0	2	100	99
7[b]	M + A	0	2	100	3

[a] $Zn(OAc)_2 = 0$ mg. [b] DMAE $\eta = 0$ μL mg^{-1}.

prior to aging (Table 1, Entry 2), demonstrating that the milling step was not prerequisite to the reaction outcome. Similarly, we found that the reactions also proceeded to 26 % conversion in absence of DBU (Table 1, Entry 3), showing that the basic catalyst was not critical to the formation of **1**, yielding ca. 2 % enhancement (Figures 1c and d). This minor increase might be due to improved reactant mobility rather than the expected catalytic effect, therefore playing no significant role in the reaction. Removing both DBU and DMAE ($\eta = 0\ \mu L\,mg^{-1}$) led to 3 % conversion, revealing that the presence of catalytic amounts of a liquid is necessary (Table 1, Entry 7). The presence of templating $Zn(OAc)_2$ was crucial for the synthesis of **1**, as the control reaction without the template did not yield any product (Table 1, Entry 4).

To speed up the reaction and improve the conversion (56 % in three weeks, Table 1, Entry 5), we increased the aging temperature from 55 to 100 °C. At this temperature, full conversion (99 %) of **2** into **1** was obtained already after 48 hours of aging (Table 1, Entry 6), although some aromatic by-products are noticeable (Figure 1d, Entry 6, between 8.0 and 7.6 ppm). Higher temperatures were not tested to avoid evaporation of the small amount of liquid from the reaction. In line with previous reports, the reaction of phthalonitriles with no inherent symmetry result in regioisomers of the corresponding ZnPc, which form a glassy amorphous product (see Figure S12).[36,61] In order to test the robustness of the optimized conditions, other liquids commonly used in LAG protocols and metal templates were tested. First, DMF results in cyclotetramerization reaction, although in lower conversion than with DMAE (79 % compared to 99 %). On the other hand, DMSO leads to heavy decomposition, and EtOH led to no reaction (see Supporting Information and Figure S9). Secondly, different metal templates were tested, employing the corresponding acetate or chloride salts (i.e. $ZnCl_2$, $Co(OAc)_2$, $CoCl_2$, $Cu(OAc)_2$, $FeCl_2{\cdot}4H_2O$, $MgCl_2$, $Mn(OAc)_2{\cdot}4H_2O$ and $MnCl_2{\cdot}4H_2O$). We observed that the Co^{2+} and Cu^{2+} acetate salts resulted in successful reaction, yielding the corresponding metal Pcs **3** and **4**. On the other hand, the Zn^{2+} and Mg^{2+}chloride salts led to **1** and **5** in lower conversions (see Table S8 and Figure S10 and S11). Other chloride salts led to no reaction, which is likely due to higher water content in the metal salts, either coordinated or adsorbed, which hinders the cyclotetramerization. To confirm the role of moisture, the reaction with $Zn(OAc)_2$ (Table 1, Entry 3) was repeated in the presence of 100 % humidity at 55 °C.[62] These conditions did not lead to a successful reaction, thus supporting the hypothesis of the negative impact of water on this reaction.

The optimized reaction conditions (Table 1, Entry 6) represent a 10-fold reduction in the volume of DMAE used, to a stoichiometric amount where it cannot be described as a solvent ($\eta = 0.192\ \mu L\,mg^{-1}$, 1.8 molar equivalents towards the product **1**). Under identical experimental set-up, the conversion was not significantly affected by scaling-up the reaction 10-fold (2.0 g of **2**, $\eta = 0.192\ \mu L\,mg^{-1}$ of DMAE, see Table S6 and Figure S8). According to the most widely proposed mechanism of Pc formation, DMAE acts as nucleophile that catalyses the Pc formation, initializing the cyclotetramerization.[14] Therefore, the solid-state synthesis of Pcs enables the study of the DMAE catalytic range. Thereafter, we screened the effect of DMAE amount on the conversion, to determine if the formation of **1** would proceed with even sub-equimolar amounts of DMAE (Figure 1e). First, it was found that aging experiments without previous ball milling (Figure 1e, blue) between DMAE contents of $\eta = 0.077$ and $0.192\ \mu L\,mg^{-1}$ (0.73–1.8 equiv) results in conversions above 80 %, comparable to those with initial milling (Figure 1e, green). However, reduction in η below $0.077\ \mu L\,mg^{-1}$ leads to a steep decrease in conversion, with a noticeable effect of the mixing technique. Adding an initial five-minute milling step before aging (Figure 1e, grey background) improved the conversion ca. 10 % below $\eta = 0.077\ \mu L\,mg^{-1}$. This is likely the consequence from improved initial mixing of the reaction mixture, i.e. even dispersion of the liquid and the solid reactants, and from the potential mechanical reduction of **2** and $Zn(OAc)_2$ particle size, both yielding more homogeneous solids for aging. Therefore, with the initial ball milling step only $\eta = 0.038\ \mu L\,mg^{-1}$ of DMAE (0.37 equiv towards **1**) was necessary to reach 69 ± 2 % conversion of **1**.

DBU is often used as basic catalyst in Pc synthesis, therefore we investigated whether the addition of a small amount ($\eta = 0.038\ \mu L\,mg^{-1}$) could improve the conversion in the sub-equimolar DMAE range (i.e. $\eta = 0$ and $0.038\ \mu L\,mg^{-1}$). Indeed, in this range addition of DBU improved the conversion of **2** to **1** (see Supporting Information, Figures S2–S7, Tables S2–S5), giving 76 % conversion with just 0.18 equiv of DMAE present ($\eta = 0.019\ \mu L\,mg^{-1}$). Fully replacing DMAE with DBU however resulted in a lower conversion 40 % than a comparable reaction with only DMAE ($\eta = 0.038\ \mu L\,mg^{-1}$, gave 69 % conversion), indicating that DMAE is a more effective catalyst in these solid-state transformations.

Finally, we studied the progression of the DMAE-catalysed solid-state reactions at sub-equimolar and above equimolar catalyst contents ($\eta = 0.077$ and $0.192\ \mu L\,mg^{-1}$, respectively) during 48 hours at 100 °C (Figure 2 and Table 2, see Supporting Information for full experimental details of the kinetic experiments). The stacked NMR spectra (Figure 2a) and the corresponding characteristic absorbance centred at 678 nm (Figure 2b and S11) shows the conversion from **2** to **1** over 48 hours and reaction yield, respectively. The conversion data is plotted on Figure 2c, showing the formation of **1** (blue) and the consumption of **2** (orange) at $\eta = 0.077\ \mu L\,mg^{-1}$ (triangular symbols) and $\eta = 0.192\ \mu L\,mg^{-1}$ of DMAE (round symbols). These show, that at the lower DMAE amount (sub-equimolar), the reaction stalls before full consumption of **2**, i.e. achieving 87 ± 1 % conversion to **1**. On the other hand, at higher DMAE amount almost full consumption of **2** is achieved already after 24 h, giving 99 ± 1 % conversion to **1**.

Since the NMR conversion is derived from the ratio between **2** and **1**, but does not take side reactions into account, UV/Vis measurements (Figure 2b) were performed to determine the total concentration of **1** in each sample by using the Lambert–Beer law, thus giving an absolute amount

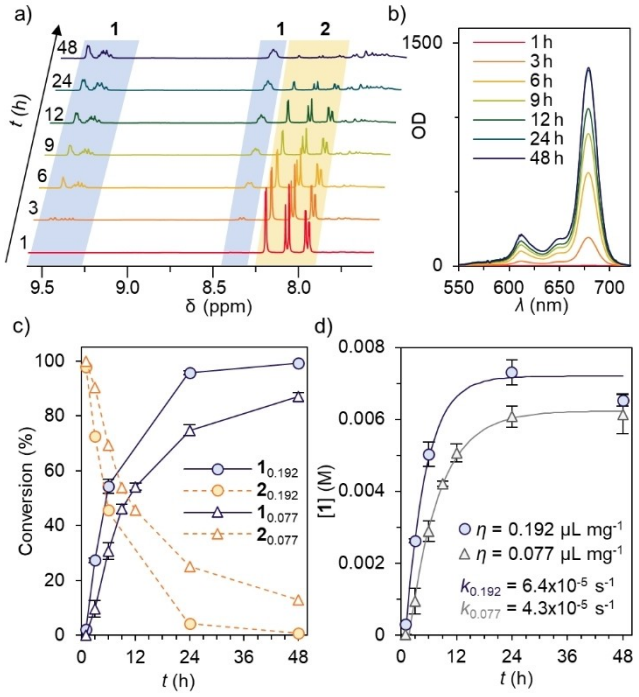

Figure 2. Time-dependent formation of **1** by milling and aging at $\eta = 0.192$ and 0.077 µL mg^{-1} over 48 h at 100 °C. a) ^{1}H NMR stacked spectra at DMAE $\eta = 0.077$ µL mg^{-1} from 1–48 h, where the decrease of **2** signals (8.2–7.7 ppm) and increase of **1** signals (9.5–8.2 ppm) is shown. Intensity is normalized to the residual solvent signal. b) UV/Vis spectra of **1**, showing the calculated optical density (OD) of the NMR samples employed for the determination of concentration of **1**. c) Conversion calculated from the integrated NMR spectra, showing the evolution of **1** (blue) and **2** (orange) at $\eta = 0.192$ and 0.077 µL mg^{-1} (circles and triangles, respectively). Data shown as the average of three independent reactions (see Supporting Information, Entries 49–51 and 52–54) ± sd. Data points are connected with lines to guide the eye and show reaction progression. d) Yield of **1** measured by UV/Vis at $\eta = 0.192$ and 0.077 µL mg^{-1} (blue and grey, respectively). Data shown as the average of three independent reactions (see Supporting Information, Entries 49–51 and 52–54) ± sd. Fitted data shown as solid line to a first-order reaction kinetics.

of Pc synthetized and the yield (Figure 2d, see Supporting Information for full experimental details). Indeed, based on the UV/Vis, while **1** is the major product formed at 62 ± 3 % and 73 ± 2 % yield for $\eta = 0.077$ µL mg^{-1} and $\eta = 0.192$ µL mg^{-1}, respectively at 48 h, the formation of **1** effectively converges within 24 h. After that, the formation of side-products is indicated by the somewhat lower yield of **1** compared to the respective conversions (Table 2) and the presence of unresolved signals in ^{1}H NMR below 7.8 ppm. The reaction rates were calculated based on fitting the absolute concentrations of **1** measured by UV/Vis (Figure 2d) to a first-order reaction model (see Supporting Information). This revealed that the reaction rates are $k = 4.3 \times 10^{-5}$ s^{-1} and $k = 6.4 \times 10^{-5}$ s^{-1} for $\eta = 0.077$ µL mg^{-1} and $\eta = 0.192$ µL mg^{-1}, respectively. As the reaction rates are relatively similar at both DMAE amounts, we can infer that the reaction mechanism is the same in both cases. Overall, we can conclude that while the higher DMAE amount $\eta = 0.192$ µL mg^{-1} leads to a higher yield (82 ± 4 %) and conversion (96 ± 1 %) of **1** after 24 h, sub-equimolar amount of DMAE $\eta = 0.077$ µL mg^{-1} also leads to a high 62 ± 3 % yield of **1** in 24 h and may thus be preferable liquid-to-solid ratio when looking to minimize the amount of DMAE used. In order to show the applicability of our approach, the solid-state synthesis conditions were also applied to cyclotetramerize electron-deficient 4-nitrophthalonitrile into **6**, which was detected by UV/Vis and by solid-state ATR-FTIR (Supporting Information, Figure S14), but due to very poor solubility the conversion could not be quantified.

Our results provide a fundamental understanding on which parameters influence the solid-state synthesis of **1**, setting the foundations for further research. We observed that the reactions progress during aging at 55 °C (26 % conversion in 7 days) although showing higher conversion rates at 100 °C (99 % conversion in 24 h). An initial ball-milling step was shown to improve the mixing of reactants at very low liquid-to-solid ratios $\eta = 0$ to 0.038 µL mg^{-1}, but did not impact the yield of **1** at higher $\eta = 0.077$ to 0.192 µL mg^{-1}. Therefore, in the studied conditions, ball milling process plays a homogenization role, and the reaction proceeds during aging. The presence of the metal template and at least 0.74 molar equivalents of DMAE ($\eta = 0.077$ µL mg^{-1}) proved to be critical for of the efficient formation of **1** (75 % conversion, 62 % yield in 24 h). At these conditions additional catalyst DBU did not lead to a significant increase of conversion. Increasing the DMAE content to 1.8 equivalents ($\eta = 0.192$ µL mg^{-1}) results in a slightly increased reaction rate and higher conversions and yields (96 % conversion, 82 % yield in 24 h). This represents a ca. 3-fold improvement in the yield of **1** compared to previously reported molten-state synthesis,[59] and in the same range as previously

Table 2: Aging time-dependant conversion of **2** into **1**. Conversion was obtained from the NMR, and yield from UV-Vis.

Aging time [h][%]	$\eta = 0.077$ µL mg^{-1} of DMAE		$\eta = 0.192$ µL mg^{-1} of DMAE	
	Conv. to **1** [%]	Yield of **1** [%]	Conv. to **1** [%]	Yield of **1** [%]
1	0 ± 0	1 ± 1	2 ± 1	3 ± 1
3	10 ± 3	10 ± 4	27 ± 1	29 ± 1
6	31 ± 3	29 ± 3	54 ± 3	56 ± 4
9	46 ± 2	43 ± 1	–	–
12	54 ± 1	51 ± 3	–	–
24	75 ± 2	62 ± 3	96 ± 1	82 ± 4
48	87 ± 1	62 ± 6	99 ± 1[a]	73 ± 2

reported yields of 85 % reported in solution.[55] Zn^{2+}, Co^{2+}, Cu^{2+}, and Mg^{2+} Pcs (**1**, **3**–**5**) could be obtained by the developed solid-state approach by using the corresponding metal templates, as well as the Zn^{2+} (tetranitro)phthalocyanine (**6**) from 4-nitrophthalonitrile. These results provide an efficient approach for the production of Pcs in a more sustainable way, by reducing the amount of the high-boiling organic solvent DMAE up to 100-fold. As the input of constant mechanical agitation proved not to be critical to reach high yields of **1**, these reactions are easily scalable and the formation mechanism during aging is expected to follow the DMAE-catalyzed mechanism previously proposed.[58] Furthermore, this approach does not rely on the solubility of precursors, being potentially adaptable for the synthesis of highly unsoluble Pc derivatives.

Acknowledgements

This work was a part of the Academy of Finland's Flagship Programme under Projects No. 318890 and 318891 (Competence Center for Materials Bioeconomy, FinnCERES). We acknowledge the funding from the Academy of Finland (341057), the Marie Sklodowska-Curie grant (101027061), and the Academy of Finland Centers of Excellence Program (2022–2029) in Life-Inspired Hybrid Materials (LIBER), project number (346110). We acknowledge the provision of facilities and technical support by Aalto University Bioeconomy and Raw Materials Research Infrastructure (RAMI) facilities.

Conflict of Interest

The authors declare no conflict of interest.

Data Availability Statement

The data that support the findings of this study are available in the Supporting Information of this article.

Keywords: Green Chemistry · Phthalocyanine · Solid-State Synthesis

[1] K. Tanaka, F. Toda, *Chem. Rev.* **2000**, *100*, 1025–1074.
[2] G. Kaupp in *Encyclopedia of Physical Organic Chemistry, Vol. 5* (Ed.: Z. Wang), Wiley, Hoboken, **2016**, pp. 1–79.
[3] V. Štrukil, M. D. Igrc, L. Fábián, M. Eckert-Maksić, S. L. Childs, D. G. Reid, M. J. Duer, I. Halasz, C. Mottillo, T. Friščić, *Green Chem.* **2012**, *14*, 2462–2473.
[4] S. L. James, C. J. Adams, C. Bolm, D. Braga, P. Collier, T. Friščić, F. Grepioni, K. D. M. Harris, G. Hyett, W. Jones, A. Krebs, J. Mack, L. Maini, A. G. Orpen, I. P. Parkin, W. C. Shearouse, J. W. Steed, D. C. Waddell, *Chem. Soc. Rev.* **2012**, *41*, 413–447.
[5] T. Friščić, C. Mottillo, H. M. Titi, *Angew. Chem. Int. Ed.* **2020**, *59*, 1018–1029; *Angew. Chem.* **2020**, *132*, 1030–1041.
[6] S. Tanaka, *Metal-Organic Frameworks for Biomedical Applications*, Elsevier, Amsterdam, **2020**, pp. 197–222.
[7] S. Kaabel, R. S. Stein, M. Fomitšenko, I. Järving, T. Friščić, R. Aav, *Angew. Chem. Int. Ed.* **2019**, *58*, 6230–6234; *Angew. Chem.* **2019**, *131*, 6296–6300.
[8] A. Krusenbaum, S. Grätz, G. T. Tigineh, L. Borchardt, J. G. Kim, *Chem. Soc. Rev.* **2022**, *51*, 2873–2905.
[9] X. Li, M. Baldini, T. Wang, B. Chen, E. Xu, B. Vermilyea, V. H. Crespi, R. Hoffmann, J. J. Molaison, C. A. Tulk, M. Guthrie, S. Sinogeikin, J. V. Badding, *J. Am. Chem. Soc.* **2017**, *139*, 16343–16349.
[10] A. P. Amrute, J. De Bellis, M. Felderhoff, F. Schüth, *Chem. Eur. J.* **2021**, *27*, 6819–6847.
[11] L. P. Jameson, S. V. Dzyuba, *Beilstein J. Org. Chem.* **2013**, *9*, 786–790.
[12] H. Lu, N. Kobayashi, *Chem. Rev.* **2016**, *116*, 6184–6261.
[13] D. Gounden, N. Nombona, W. E. van Zyl, *Coord. Chem. Rev.* **2020**, *420*, 213359.
[14] M. O. Senge, N. N. Sergeeva, K. J. Hale, *Chem. Soc. Rev.* **2021**, *50*, 4730–4789.
[15] E. Anaya-Plaza, J. Joseph, S. Bauroth, M. Wagner, C. Dolle, M. Sekita, F. Gröhn, E. Spiecker, T. Clark, A. Escosura, D. M. Guldi, T. Torres, *Angew. Chem. Int. Ed.* **2020**, *59*, 18786–18794; *Angew. Chem.* **2020**, *132*, 18946–18955.
[16] G. Bottari, O. Trukhina, M. Ince, T. Torres, *Coord. Chem. Rev.* **2012**, *256*, 2453–2477.
[17] G. Bottari, G. de la Torre, D. M. Guldi, T. Torres, *Coord. Chem. Rev.* **2021**, *428*, 213605.
[18] G. Bottari, G. de La Torre, D. M. Guldi, T. Torres, *Chem. Rev.* **2010**, *110*, 6768–6816.
[19] E. Anaya-Plaza, A. Aljarilla, G. Beaune Nonappa, J. V. I. Timonen, A. Escosura, T. Torres, M. A. Kostiainen, *Adv. Mater.* **2019**, *31*, 1902582.
[20] E. Anaya-Plaza, E. van de Winckel, J. Mikkilä, J.-M. Malho, O. Ikkala, O. Gulías, R. Bresolí-Obach, M. Agut, S. Nonell, T. Torres, M. A. Kostiainen, *Chem. Eur. J.* **2017**, *23*, 4320–4326.
[21] A. Shaukat, E. Anaya-Plaza, S. Julin, V. Linko, T. Torres, A. De La Escosura, M. A. Kostiainen, *Chem. Commun.* **2020**, *56*, 7341–7344.
[22] V. Almeida-Marrero, E. van de Winckel, E. Anaya-Plaza, T. Torres, A. de la Escosura, *Chem. Soc. Rev.* **2018**, *47*, 7369–7400.
[23] M. Urbani, G. de la Torre, M. K. Nazeeruddin, T. Torres, *Chem. Soc. Rev.* **2019**, *48*, 2738–2766.
[24] M. Urbani, M. Ragoussi, M. K. Nazeeruddin, T. Torres, *Coord. Chem. Rev.* **2019**, *381*, 1–64.
[25] T. M. Grant, D. S. Josey, K. L. Sampson, T. Mudigonda, T. P. Bender, B. H. Lessard, *Chem. Rec.* **2019**, *19*, 1093–1112.
[26] M. Wang, K. Torbensen, D. Salvatore, S. Ren, D. Joulié, F. Dumoulin, D. Mendoza, B. Lassalle-Kaiser, U. Işci, C. P. Berlinguette, M. Robert, *Nat. Commun.* **2019**, *10*, 3602.
[27] S. Yamazaki, *Coord. Chem. Rev.* **2018**, *373*, 148–166.
[28] A. B. Sorokin, *Chem. Rev.* **2013**, *113*, 8152–8191.
[29] G. Guillaud, J. Simon, J. P. Germain, *Coord. Chem. Rev.* **1998**, *178–180*, 1433–1484.
[30] A. Galstyan, *Chem. Eur. J.* **2021**, *27*, 1903–1920.
[31] B. Zheng, Q. He, X. Li, J. Yoon, J. Huang, *Coord. Chem. Rev.* **2021**, *426*, 213548.
[32] P. Lo, M. S. Rodríguez-Morgade, R. K. Pandey, D. K. P. Ng, T. Torres, F. Dumoulin, *Chem. Soc. Rev.* **2020**, *49*, 1041–1056.
[33] R. C. H. Wong, P. C. Lo, D. K. P. Ng, *Coord. Chem. Rev.* **2019**, *379*, 30–46.
[34] X. Li, B. Zheng, X. Peng, S. Li, J. Ying, Y. Zhao, J.-D. Huang, J. Yoon, *Coord. Chem. Rev.* **2019**, *379*, 147–160.
[35] Y. Zhang, J. F. Lovell, *WIREs Nanomed. Nanobiotechnol.* **2017**, *9*, e1420.

[36] G. Zanotti, P. Imperatori, A. M. Paoletti, G. Pennesi, *Molecules* **2021**, *26*, 1760.
[37] F. Cong, H. Jiang, X. Du, W. Yang, S. Zhang, *Synthesis* **2021**, *53*, 2656–2664.
[38] H. Tomoda, S. Saito, S. Ogawa, S. Shiraishi, *Chem. Lett.* **1980**, *9*, 1277–1280.
[39] G. Dede, R. Bayrak, M. Er, A. R. Özkaya, İ. Değirmencioğlu, *J. Organomet. Chem.* **2013**, *740*, 70–77.
[40] B. I. Kharisov, U. Ortiz Méndez, J. L. Almaraz Garza, J. R. Almaguer Rodríguez, *New J. Chem.* **2005**, *29*, 686–692.
[41] X. Li, Y. Feng, C. Li, H. Han, X. Hu, Y. Ma, Y. Yang, *Green Process. Synth.* **2021**, *10*, 95–100.
[42] K. Zhu, C. Wang, J. Liu, W. Wang, Y. Lv, P. Wang, A. Meng, Z. Li, *J. Asian Ceram. Soc.* **2020**, *8*, 939–947.
[43] S. Zhang, H. Zhang, X. Hua, S. Chen, *J. Mater. Chem. A* **2015**, *3*, 10013–10019.
[44] W. Mekprasart, N. Vittayakorn, W. Pecharapa, *Mater. Res. Bull.* **2012**, *47*, 3114–3119.
[45] W. Mekprasart, W. Jarernboon, W. Pecharapa, *Mater. Sci. Eng. B* **2010**, *172*, 231–236.
[46] M. Wang, H. Shi, P. Zhang, Z. Liao, M. Wang, H. Zhong, F. Schwotzer, A. S. Nia, E. Zschech, S. Zhou, S. Kaskel, R. Dong, X. Feng, *Adv. Funct. Mater.* **2020**, *30*, 2002664.
[47] T. Chen, B. Liu, *Mater. Lett.* **2017**, *209*, 467–471.
[48] L. Cao, X. Fei, H. Zhao, C. Huang, *Dyes Pigm.* **2020**, *173*, 107879.
[49] Z. Chen, X. Wang, W. Lang, D. Qi, *RSC Adv.* **2019**, *9*, 32490–32498.
[50] Q. Xiao, C. Zhan, Y. You, L. Tong, R. Wei, X. Liu, *Mater. Lett.* **2018**, *227*, 33–36.
[51] O. A. Hakeim, H. A. Diab, J. Adams, *Prog. Org. Coat.* **2015**, *84*, 70–78.
[52] G. Kaupp, *CrystEngComm* **2009**, *11*, 388–403.
[53] G. A. Bowmaker, *Chem. Commun.* **2013**, *49*, 334–348.
[54] I. Huskić, C. B. Lennox, T. Friščić, *Green Chem.* **2020**, *22*, 5881–5901.
[55] J. U. Lee, Y. Do Kim, J. W. Jo, J. P. Kim, W. H. Jo, *J. Mater. Chem.* **2011**, *21*, 17209–17218.
[56] C. E. Dent, R. P. Linstead, *J. Chem. Soc.* **1934**, 1027.
[57] R. P. Linstead, A. R. Lowe, *J. Chem. Soc.* **1934**, 1022.
[58] R. M. Christie, D. D. Deans, *J. Chem. Soc. Perkin Trans. 2* **1989**, 193.
[59] L.-C. Liu, C.-C. Lee, A. Teh Hu, *J. Porphyrins Phthalocyanines* **2001**, *05*, 806–807.
[60] T. Friščić, S. L. Childs, S. A. A. Rizvi, W. Jones, *CrystEngComm* **2009**, *11*, 418–426.
[61] Q. Hu, E. Rezaee, L. Dong, Q. Dong, H. Shan, Q. Chen, M. Li, S. Cai, L. Wang, Z.-X. Xu, *Sol. RRL* **2019**, *3*, 1900182.
[62] In order to avoid the boiling point of EtOH.

Manuscript received: June 20, 2022
Accepted manuscript online: July 25, 2022
Version of record online: August 16, 2022